PROCEEDINGS OF SPIE

SPIEDigitalLibrary.org/conference-proceedings-of-spie

Design and development of WFOS, the Wide-Field Optical Spectrograph for the Thirty Meter Telescope

Charles Steidel, Eric Peng, Jason Fucik, Reston Nash, Stephen Kaye, et al.

Charles Steidel, Eric Peng, Jason Fucik, Reston Nash, Stephen Kaye, George Jacoby, Bernard Delabre, Ramya Sethuram, Devika Divakar, Hari Mohan Varshney, Thirupathi Sivarani, Fumihiro Uraguchi, Shinobu Ozaki, Hangxin Ji, Tao LV, Kent Chiu, Qinfeng Zhu, David Andersen, John Miles, Davide Lasi, "Design and development of WFOS, the Wide-Field Optical Spectrograph for the Thirty Meter Telescope," Proc. SPIE 12184, Ground-based and Airborne Instrumentation for Astronomy IX, 1218423 (29 August 2022); doi: 10.1117/12.2629464

SPIE.

Event: SPIE Astronomical Telescopes + Instrumentation, 2022, Montréal, Québec, Canada

Design and Development of WFOS, the Wide-Field Optical Spectrograph for the Thirty Meter Telescope

Charles Steidel[a], Eric Peng[b], Jason Fucik[a], Reston Nash[a], Stephen Kaye[a], George Jacoby[c], Bernard Delabre[c], Ramya Sethuram[d], Devika Divakar[d], Hari Mohan Varshney[e], Sivarani Thirupathi[e], Fumihiro Uraguchi[f], Shinobu Ozaki[f], Hangxin Ji[g], Tao LV[h], Kent Chiu[i], Qingfeng Zhu[i], David Andersen[c], John Miles[c], and Davide Lasi[c]

[a]California Institute of Technology, USA
[b]Peking University, China
[c]TMT International Observatory, USA
[d]India TMT Coordination Centre, India
[e]Indian Institute of Astrophysics, India
[f]National Astronomical Observatory of Japan
[g]National Astronomical Observatory of China - Nanjing Institute of Astronomical Optics and Technology, China
[h]Xi'an Institute of Optics and Precision Mechanics, China
[i]University of Science and Technology of China

ABSTRACT

We present the current design of WFOS, a wide-field UV/optical (0.31-1.0 μm) imaging spectrograph planned for first-light on the TMT International Observatory 30 m telescope. WFOS is optimized for high sensitivity across the entire optical waveband for low-to-moderate resolution (R $\sim$ 1500-5000) long-slit and multi-slit spectroscopy of very faint targets over a contiguous field of view of $8\farcm3\times3\farcm0$ at the f/15 Nasmyth focus of TMT. A key design goal for WFOS is stability and repeatability in all observing modes, made possible by its gravity-invariant opto-mechanical structure, with a vertical rotation axis and all reconfigurable components moving only in planes defined by tiered optical benches parallel to the Nasmyth platform. WFOS's optics include a linear ADC correcting a 9′ diameter field, including both the science FoV and 4 patrolling acquisition, guiding, and wavefront sensing camera systems; a novel 2-mirror reflective collimator allowing the science FoV to be centered on the telescope optical axis; a dichroic beamsplitter dividing the collimated beam into 2 wavelength-optimized spectrometer channels (blue: 0.31-0.56 μm; red: 0.54-1.04 μm); selectable transmissive dispersers (VPH and/or VBG) with remotely configurable grating tilt (angle of incidence) and camera articulation that enable optimization of diffraction efficiency and wavelength coverage in each channel; all-refractive, wavelength-optimized f/2 spectrograph cameras, and UV/blue and red-optimized detector systems. The predicted instrumental throughput of WFOS for spectroscopy averages $>$ 56% over the full 0.31-1 μm range, from the ADC to the detector. When combined with the 30 m TMT aperture, WFOS will realize a factor of $\sim$20 gain in sensitivity compared to the current state of the art on 8-10 m-class telescopes.

Keywords: Instrumentation, Spectrograph, TMT, UV/optical, multi-slit spectrometer

1. OVERVIEW

WFOS is an imaging spectrograph designed to perform multi-object spectroscopy, single object spectroscopy, or direct imaging of very faint sources throughout the optical waveband (0.31-1.0 μm) using seeing-limited or ground-layer AO-corrected images delivered by the Thirty Meter Telescope (TMT). It is designed to have very high instrumental throughput in order to preserve the aperture advantage of TMT relative to current-generation multi-object spectrographs on 8-10m telescopes. WFOS obtains images or spectra using single or multi-slit focal

Send correspondence to: ccs@astro.caltech.edu

Ground-based and Airborne Instrumentation for Astronomy IX, edited by Christopher J. Evans, Julia J. Bryant, Kentaro Motohara, Proc. of SPIE Vol. 12184, 1218423

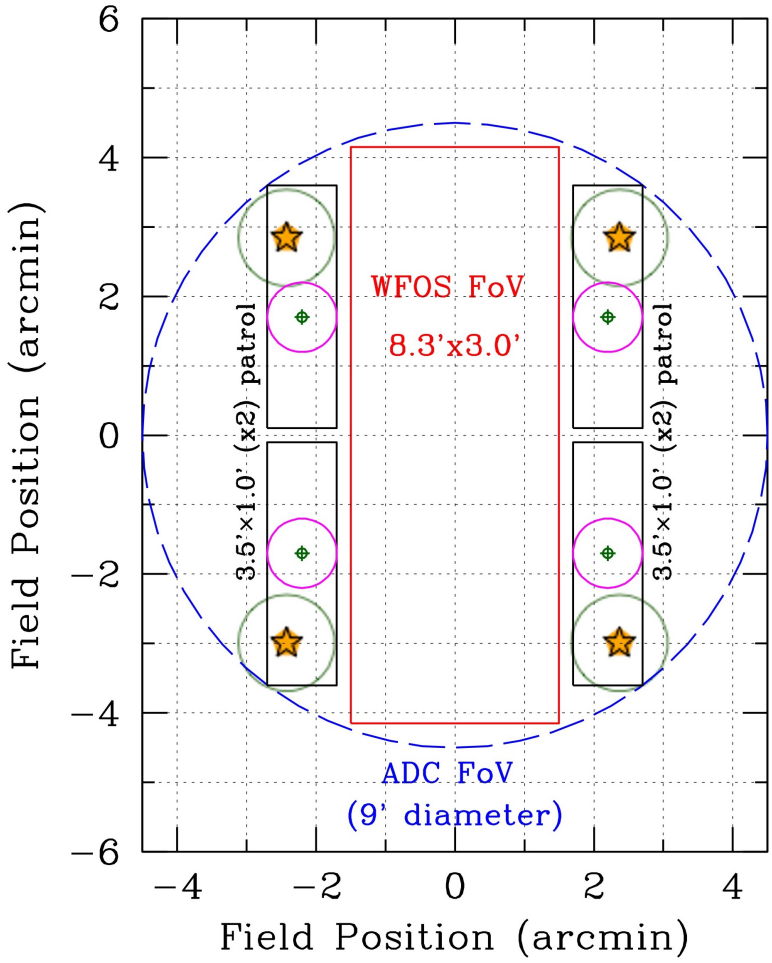

Figure 1: The WFOS field of view in the f/15 TMT focal plane. Labels correspond to dimensions projected onto the plane of the sky in units of arc minutes, with the origin at the telescope optical axis. The 8.′3 by 3.′0 WFOS science field (red rectangle) is flanked by 4 patrolling acquisition and guide cameras (AGC) for field acquisition and guiding; each has a patrol range of 3.′5 and an instantaneous field of view of 60″ in diameter (example camera positions indicated with magenta circles). The dashed blue circle indicates the FoV corrected by the linear ADC (9′ diameter); the small green circles with crosses inside each AG camera FoV represent Low Order WaveFront Sensor (LOWFS) pickoff probes that can move anywhere in the AG camera field of view to acquire a star for continuous wavefront sensing. Green circles with yellow stars indicate the field positions of the Laser Guide Star (LGS) asterism for wide-field Ground-Layer Adaptive Optics (GLAO) produced by the TMT facility laser launch system (see §2.)

plane masks placed within a contiguous rectangular field of view of 8.′3×3.′0 (Fig. 1), for a total slit length of 500″ and field area of 25 arcmin^2. The sensitivity and multiplex of WFOS is motivated by a wide range of astrophysical studies, including tomography of the intergalactic medium, the star-formation and chemical enrichment histories of galaxies, and the chemical composition of exoplanet atmospheres. These science cases require a versatile range of spectral resolution across the full optical wavelength range, and the ability to cover the full wavelength range at $R \sim 1500$ in a single exposure.

The WFOS structure will occupy a fixed location on TMT's +X Nasmyth platform, fed directly at the nominal f/15 focus by the telescope tertiary mirror (M3), which is articulated to provide access to other permanently mounted instruments on either Nasmyth platform. As illustrated in Fig. 2, the beam from M3 passes through a linear Atmospheric Dispersion Corrector (ADC; §3.1) system, after which it is re-directed by a fold mirror (M4) so that the telescope focal surface is up-looking, and the optical axis of the instrument is perpendicular to the Nasmyth platform. Long-slit or multi-slit masks are inserted into the vertical beam at the focal surface. The images of the slit plane are then collimated over the full 8.′3×3.′0 science field of view by a novel two-mirror reflecting collimator system (§3.3) with an effective focal length of $\simeq$ 4.5 m, forming a 300 mm beam that is divided into blue (0.31-0.58 μm) and red (0.54-1.05 μm) channels by a dichroic beamsplitter with the wavelength split near 0.56 μm. After the collimator and dichroic beam splitter, a fold mirror in each wavelength channel directs the beam to form a pupil image, near to which one may insert a Volume Phase Holographic (VPH) or Volume Binary Grating (VBG) dispersive element (or any other transmissive grating) for spectroscopy. Gratings are removed from the beam to allow direct imaging over the same field of view. The dispersed light (or direct images) emerging from the grating/filter are re-imaged by blue and red camera systems with focal lengths of

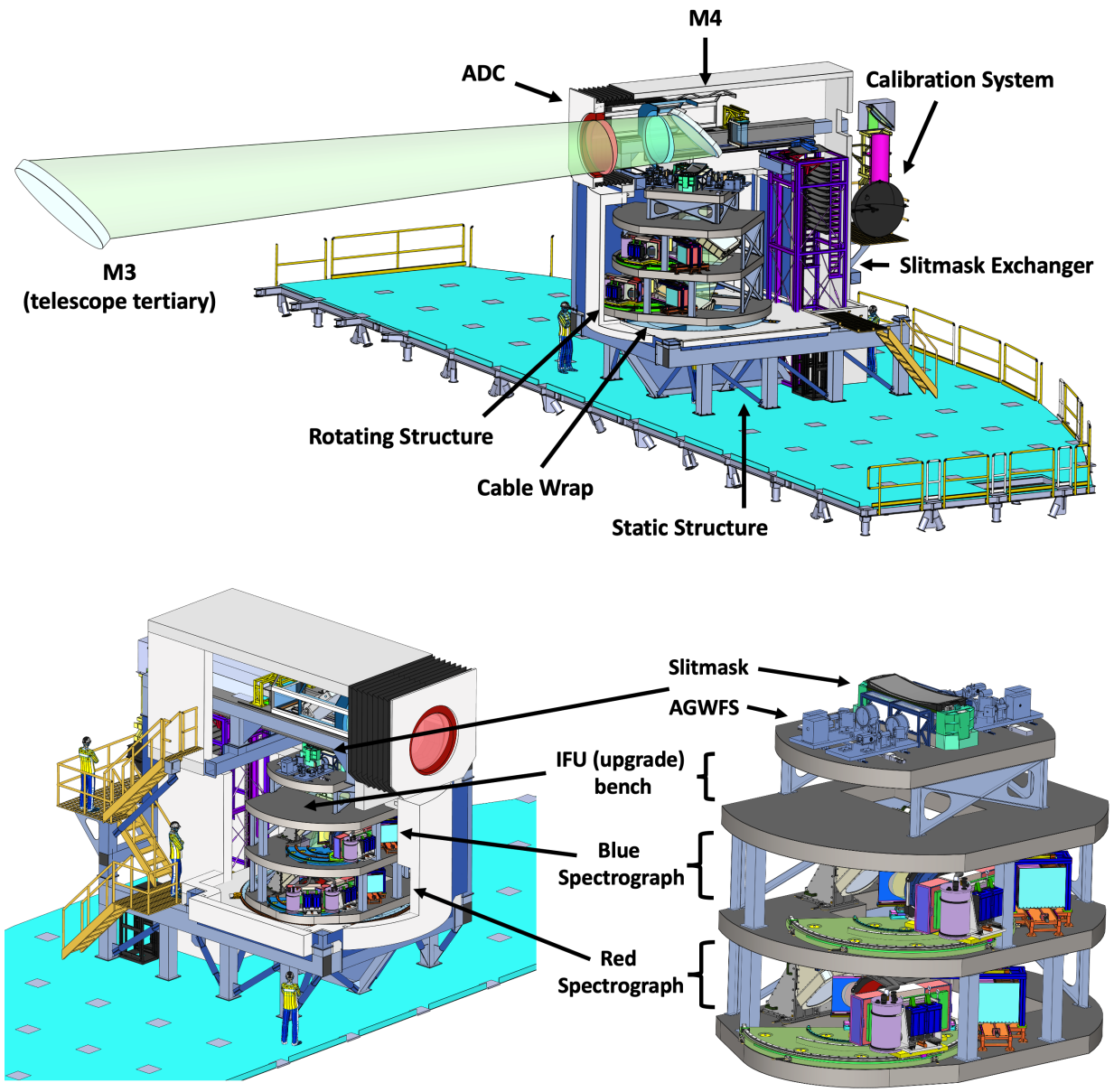

Figure 2: Overview of the WFOS opto-mechanical layout.

$\simeq$ 0.6 m. Intermediate or broadband filters (which may be used for imaging or as band-limiting filters in spectroscopic mode) are placed in the converging f/2 beam within the camera systems*. An illustration of the current WFOS optical layout is given in Fig. 4.

With no slit mask inserted at the telescope focal surface, an image of the full science field of view is formed at the focus of each spectrometer camera, reduced in scale by a factor of $F_{\rm coll}/F_{\rm cam} \simeq 4.5{\rm m}/0.6{\rm m} \simeq 7.5$, for a plate scale at the detector focal plane of 291 μm/$''$, or $\simeq 0''.052$ per 15 μm pixel. Thus, the direct imaging field of view on the detector mosaic has a physical size of $\sim 145.3 \times 52.3$ mm (see Fig. 3). For spectroscopy, the image of the illuminated slitmask at the telescope focal surface is collimated and presented to the grating, and the cameras focus the *dispersed* images of the mask onto the detector.

*It is also possible to insert a filter in the parallel beam near the pupil, in place of (or in addition to) a grating. Such a location may be desired for filters with < 100 Å bandwidth.

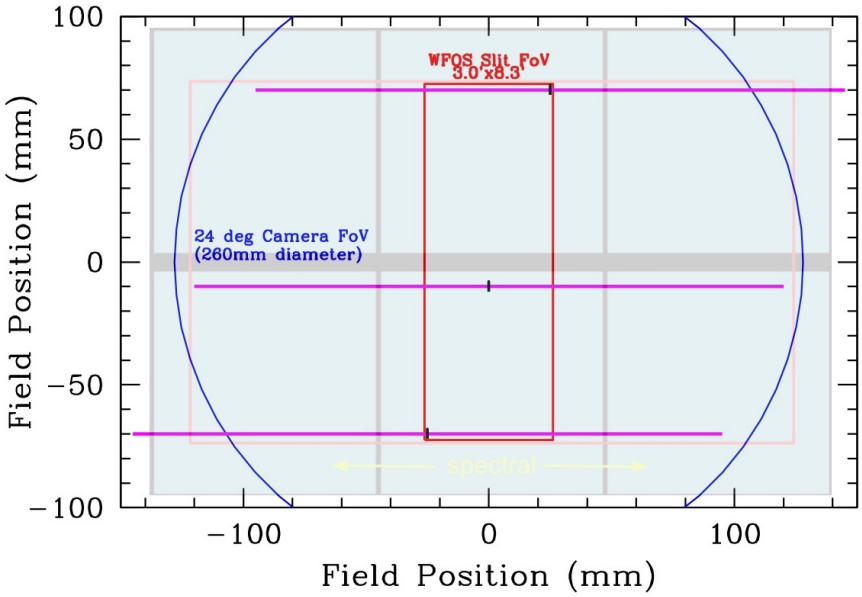

Figure 3: Map of the WFOS detector focal plane. The 6 light-blue squares are placeholder 6k×6k CCDs, the blue circle corresponds to the 24 degree camera field of view, and the red rectangle is the footprint at the camera focus of the WFOS field of view over which slits can be placed (which is the same as the FoV for direct imaging). The magenta horizontal lines show the locations of example dispersed spectra of length 240mm for slits placed near the center of the field and at two extreme field positions–indicated by the black vertical marks at the center of each spectrum. Note that direct images would be captured entirely on the 2 central CCDs for this particular CCD mosaic. The spectra would cover the wavelength ranges indicated in in Table 1 except at the most extreme field positions, where the spectral coverage is reduced by $\simeq 10\%$ at either the blue or the red end (depending on slit location in focal plane).

The camera systems have been designed with an angular field of view of 24°, driven by the desire to image as much of the dispersed spectra coming off the gratings as possible. The cameras see a field of view of ∼256 mm in diameter, thus can capture spectra up to ∼250 mm in length for slits centered in the field of view (see Fig. 3.) A typical slit of angular width $0\farcs75$ will map to $0.75/0.052 \simeq 14.4$ detector pixels (assuming 15 μm pix^{-1}). The narrowest anticipated slit width of $0\farcs25$ (possibly common if GLAO is available in the future) will have a re-imaged width of 4.8 pixels, or $\simeq 72$ μm at the detector. That is, the line spread function for the narrowest entrance apertures anticipated ($0\farcs25$) would produce spectra with nominal resolving power of $R \simeq 4500$ in low-resolution mode, $\gtrsim 10,000$ in medium resolution mode, and $\gtrsim 15,000$ in the high resolution mode (see grating options in Table 1) and will remain comfortably over-sampled at the detector.

WFOS will be equipped with four identical acquisition and guide cameras (AGC) placed just outside the science field of view (see Fig. 1), discussed in more detail below (§2). Each AGC unit has a conventional guide camera with instantaneous field of view of $60''$ in diameter, and is capable of patrolling along a single-axis stage over a region corresponding to $3\farcm5$ on the sky. Each AGC unit is also equipped with a low-order Shack-Hartmann wavefront sensor system covering a smaller field of view that can be directed to any suitable star within the larger AGC field of view. All 4 AGCs are used for fine acquisition of multi-slit masks, after which one or more are used for guiding during science observations, and output from one or more of the low-order wavefront-sensing systems is used by the telescope control system to maintain the focus and collimation of the telescope optics during observations.

2. ACQUISITION, GUIDING, AND WAVEFRONT SENSING SYSTEM

One of the primary design goals for WFOS has been to maximize throughput while minimizing scattered light within the science field of view to allow for the best possible control over systematics that affect background subtraction, since essentially all observations with TMT/WFOS will be background-limited. Experience has shown that including larger apertures (usually boxes with widths significantly larger than those of science slits)

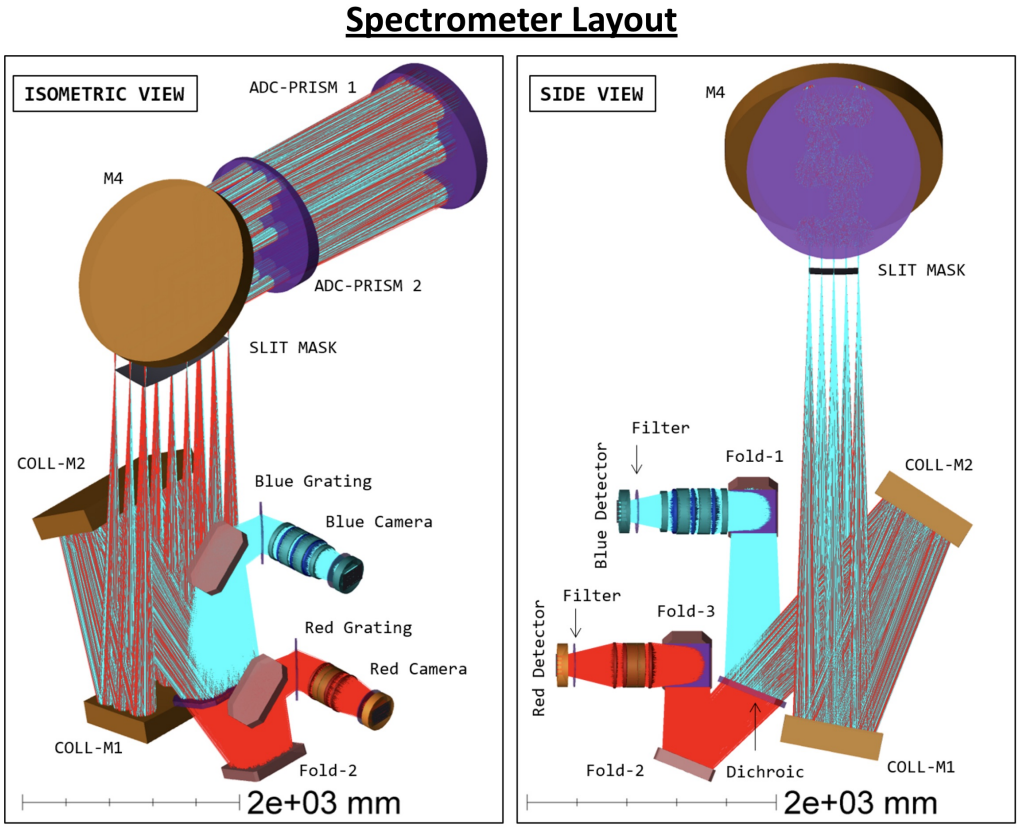

Figure 4: WFOS optical path layout for the 2-channel spectrometer design. *Left:* an isometric view of the optical components starting from the linear ADC and ending at the detector. *Right:* a side-view of the optical components. Both panels show the position of gratings and cameras in a medium-resolution ($R \sim 3500$) mode.

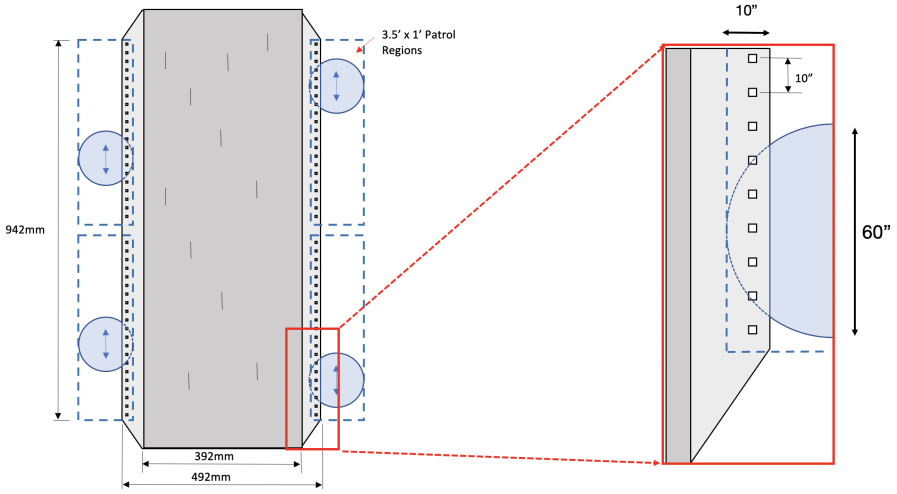

Figure 5: Schematic illustration of the concept for reference features on slit-masks beyond the science field of view, which would be recorded in the inner portions of each AGWFS camera field of view. The left-hand diagram shows the focal plane layout, including the fields of view of the AGWFS cameras. The right-hand diagram is a zoomed version of the lower right-hand corner to show the features ($1''$ boxes separated by $10''$) that would produce illuminated features in the AGWFS images that would be recorded at the same time as celestial objects over the rest of the FoV.

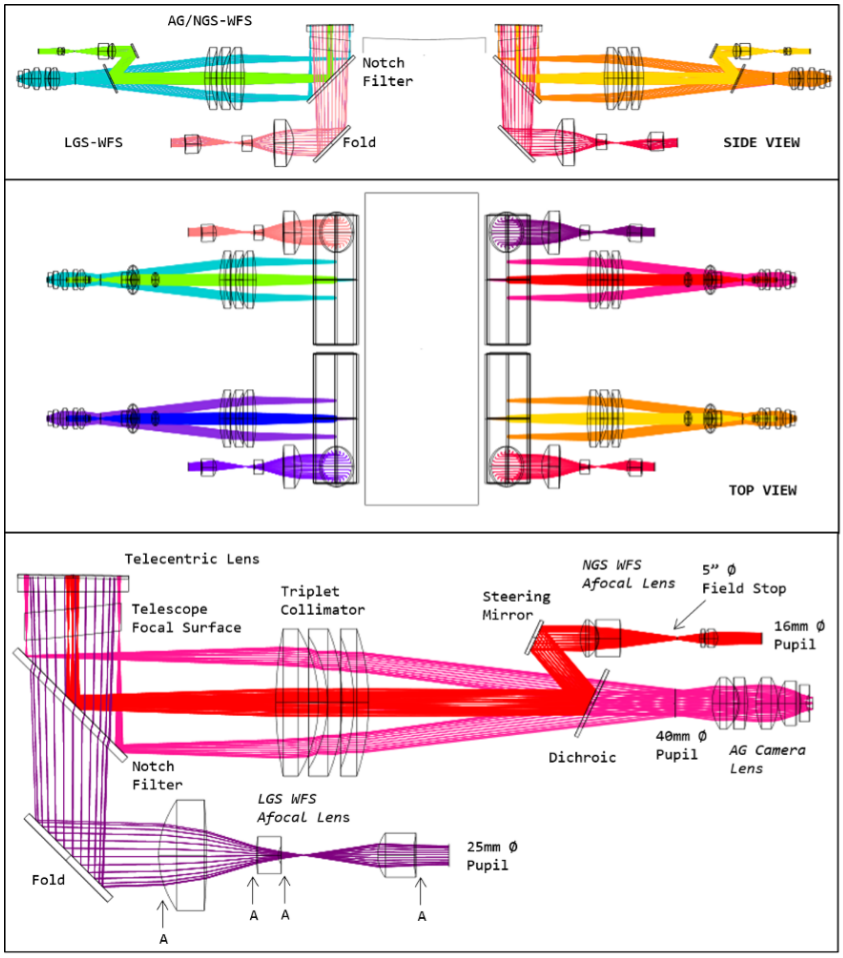

Figure 6: Side and top views of the AGWFS system for all 4 patrol fields along with an optical layout of the AGWFS system. "A" indicates an aspheric surface. The AGWFS system is composed of the NGS and LGS WFS afocal lenses and the AG camera lens.

to facilitate fine acquisition of target fields become a very significant source of scattered light for observations of very faint targets using multi-slit masks. For this reason, and in order to streamline the process of fine acquisition during nighttime observations, WFOS plans to use the four patrolling AGC systems that view regions of the sky just outside the science FoV to establish the astrometric connection between celestial objects and the metrology of the TMT f/15 focal surface. This means that both wavelength channels can be configured for the next observation during a telescope slew (i.e. there is no need to place either channel into direct imaging mode in order to image through the slit mask for acquisition and fine alignment), while the AGC systems are being positioned to predetermined stage positions that place an ensemble of celestial reference objects (e.g. Gaia catalog stars) within the $4\times$ $60''$ diameter fields of view of the AGCs. Fine alignment requires solving for small offsets in telescope pointing and rotation of the instrument that will align targets with their slits. This is accomplished by analyzing short exposures on the guide cameras. The current slitmask concept has the ability to ensure the registration of the mechanical coordinate system of the slitmasks with the celestial coordinate system of the AGC cameras by including physical reference features on the masks (see Fig. 5) located outside of the science field of view, but imaged by the patrolling guide cameras.

Once fine alignment is established using the AG cameras, science observations can begin immediately, without needing to reconfigure the instrument from imaging to spectroscopy mode. Guiding is accomplished using any of the 4 AG cameras; each AGC also allows for positioning of a small tip/tilt mirror to send light from a selected star (which may be the same star used for telescope guiding) into a low order Shack-Hartmann wavefront sensor (7×7 sub-apertures in the current design) for maintaining telescope focus during observations. The current optical layout of the AGWFS systems, including notional laser guide star wavefront sensor systems, is shown in Fig. 6.

3. OPTO-MECHANICAL DESIGN

3.1 Atmospheric Dispersion Corrector (ADC)

WFOS is designed to work from the atmospheric cutoff in the near-UV (310 nm on Maunakea) to > 1 μm where the amplitude of differential refraction from the atmosphere is as much as $\simeq 3''$ for a zenith angle of 60° (airmass = 2.0). An ADC is essential when using narrow entrance slits at arbitrary angles with respect to parallactic without incurring wavelength-dependent slit losses. The size of the instrument field of view at the telescope focal surface requires a corrected field with an angular diameter projected onto the sky of $9'.0$ (see Fig. 1, or a physical diameter of > 1.2 m. Its location in the converging f/15 beam prior to the telescope focal surface requires a clear aperture of ~ 1.4 m diameter.

WFOS has adopted a linear ADC design, similar in concept to the Cassegrain ADC on the Keck 1 telescope,[1] composed of two ~ 1.4 m diameter fused silica prisms with apex angles of $7.^{\circ}6$, mounted on translation and rotation drive mechanisms to correct for the elevation-dependent refraction, where the pair of prisms must also track the rotation of the elevation direction with respect to the sky position angle of the observation. The prism axial separation is adjusted as a function of the telescope elevation angle, from zero at zenith to a maximum separation of $\sim$2 m. As designed, the ADC ensures that polychromatic images over the operational wavelength range of WFOS show residual lateral color of $< 0''.2$ for ZD $\leq 60°$.

3.2 Fold Mirror (M4)

A fold mirror (M4) positioned directly after the ADC directs light coming from the telescope tertiary downward by 90° . This orients the optical axis perpendicular to the Nasmyth platform, allowing all downstream spectrograph components to operate in a gravity-invariant environment. M4 is a 1.8 m diameter flat mirror mounted to the stationary structure of the instrument. It has two rotational positions: one receives light from the telescope and ADC for nighttime observations, and a second – achieved with a 90-degree rotation of M4 – receives light from the calibration system (§5, Fig. 12.) The M4 mount also enables tip/tilt control of the mirror surface that is used to correct for small shifts in the instrument pupil position that depend on the rotation and axial separation of the ADC prisms.

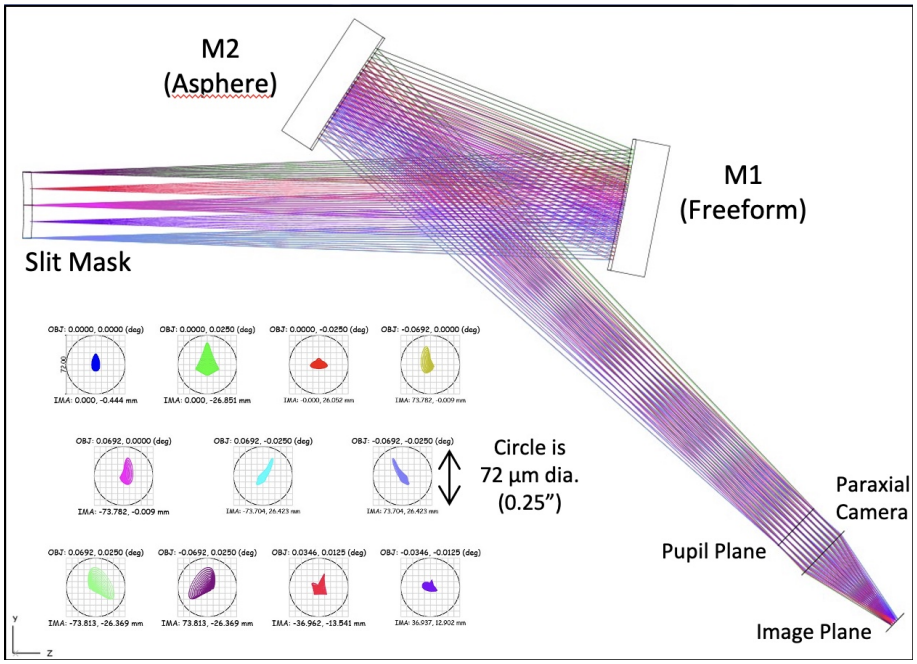

Figure 7: Schematic diagram of the 2-mirror reflective collimator optical design.

3.3 Collimator

The collimator is designed to collimate light from the telescope and form an image of the telescope primary mirror (entrance pupil). The instrument pupil then provides a location in the instrument to position a dispersive element such as a grating for spectroscopy. The WFOS collimator is an on-axis 2-mirror reflective design incorporating freeform and aspheric surfaces. The 2-mirror solution adopts principles from a Tilted Component Telescope (TCT, or "Schiefspiegler") designs 2. The collimator prescription balances mechanical volume constraints and image quality by adjusting the mirror spacing and tilt (see Fig. 7). The two surfaces are on-axis, but tilted by 11° to avoid any obstruction between the mirrors and light paths. The first mirror after the slit mask is a free-form surface with corrections for astigmatism, coma, and spherical aberrations. The mirror is 1.50 x 0.80 m physical size (1.25 x 0.65 m CA) that will be fabricated from a low expansion ceramic material (e.g. Zerodur). The second mirror is an aspheric surface with a fourth order (r^4) corrective term. The mirror also has a 1.50 x 0.80 m physical size (1.42 x 0.70 m CA).

The collimator couples the f/15 beam from the telescope to the spectrometer. The angles exiting the collimator pupil must yield a reasonable range that can be handled by a Petzval style refractive camera with a f/2 focal ratio that can maintain good aberration control. The pupil diameter must also be large enough to achieve the desired range of spectral resolution for the spectrometer. A collimator focal length of 4.5 m was selected that forms a 300 mm pupil diameter. With a 4.5 m focal length, the field angles exiting the pupil are within an angular diameter of 15° in the spatial direction and $< 24°$ when the light is dispersed. In the spectral direction, the passband of the low-resolution (R$\sim$ 1500) spectrum is captured by the camera lens in both channels.

The 2-mirror on-axis design deviates from the commonly-used Off-Axis Parabola (OAP) collimator design used in other imaging spectrographs on Ritchey-Chrétien Telescopes (e.g. DEIMOS, LRIS, ESI at Keck Observatory). A reflective collimator is a natural design choice given the concave focal surface curvature of an RC telescope. A single OAP mirror uses an off-axis field center; previous WFOS designs had the center of the instrument axis 4.′8 from the telescope optical axis, which placed the outermost corners of the instrument field at 7.′5 radial distance from the telescope optical axis. At this field position the telescope has residual coma and astigmatism giving rms spot diameters of 0.″25. In contrast, the on-axis collimator places the corners of the field at 4.′4 radial distance where the rms spot diameter of the telescope is <0.″08. An on-axis collimator delivers significantly better telescope images and is more compatible with a GLAO system across the FoV. An OAP also has the downside that it positions the image surface near the pupil plane and can be opto-mechanically more challenging to package. The on-axis collimator removes this constraint and provides more physical area around the slit mask (focal surface) to position the AGWFS system necessary for field acquisition supporting the Telescope Control System (TCS).

3.4 Spectrograph Cameras

The spectrograph cameras are designed to have focal lengths of $\sim$ 600 mm and when paired with the collimator, de-magnifies the telescope focal surface by 7.5×. The resulting plate scale at the detector plane is 291 μm/″ (or 0.″052 per 15 μm pixel). A typical slit of angular width 0.″75 will project to a width of 14.4 pixels on the detector; the narrowest anticipated slit width of 0.″25 will have a width of 4.8 pixels. It is foreseen that the detector array will normally be binned 2×2 on the detector mosaic, so that even the narrowest slit of 0.″25 will be sampled with $\sim$ 2.4 binned pixels in the dispersion direction.

The camera barrels will be mounted on articulation stages with centers of rotation located at the grating center. The camera articulation allows the camera axis to be adjusted to any angle between 0° to 100° depending on the spectrograph configuration: 0° is used for direct imaging (i.e. no dispersion) and 30°-90°is used for spectroscopy. In combination with control over the central field point AOI on the grating that maximizes the diffraction efficiency for a given center wavelength, the camera articulation gives control over the range of dispersion angles captured by the cameras (i.e. wavelength range). A similar two-channel spectrometer layout with remote control of both camera articulation and grating tilt in each channel has been used by the KCWI instrument at Keck Observatory 3.

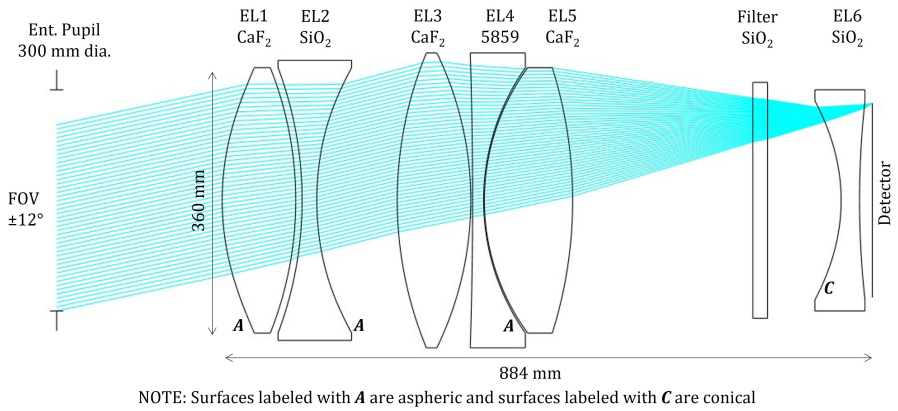

Figure 8: Optical layout of the WFOS blue spectrograph camera prescription.

3.4.1 Blue Camera (310-580 nm)

The blue camera lens design (Fig. 8) is composed of three glass materials: Calcium Fluoride (CaF_2), Fused Silica (SiO_2), and Nikon 5859 i-line glass. CaF_2 and SiO_2 glass materials are both available in ~ 400 mm diameter blank sizes and provide excellent transmission into the UV down to 310 nm; Nikon 5859 is commercially available in blank sizes up to 280 mm diameter and discussions with Nikon about developing custom blank sizes up to 400 mm in diameter are on-going. The addition of the Nikon 5859 glass, which has a higher index and abbé number than CaF_2 and SiO_2, has allowed for a camera prescription with a reduced number of elements and better control of chromatic aberrations out to $\sim$650 nm. Previous optical prescriptions using only CaF_2 and SiO_2 had 8 lens elements (instead of 6), and chromatic aberrations limited the image quality longward of ~ 530 nm. The adopted camera design has three aspheric surfaces, with maximum aspheric deviation of 1.5 mm, 0.4 mm, and 0.1 mm on lens elements 1, 2, and 4, respectively. The camera has an entrance aperture diameter of 360 mm and is ~ 900 mm in length from the front surface vertex to the detector plane. The camera delivers 80% Encircled Energy (EE80) diameters < 54 μm ($0''.19$) over an angular field of 24° for wavelengths ranging from 310 to 650 nm. The maximum geometric vignetting is $\sim 15\%$ at a field radius of 12°for a 300 mm circular pupil. The blue camera has a passband average transmission of $\sim 91\%$ including bulk material absorption losses and Fresnel losses (assuming a 0.5% loss per surface).

3.4.2 Red Camera (540-1050 nm)

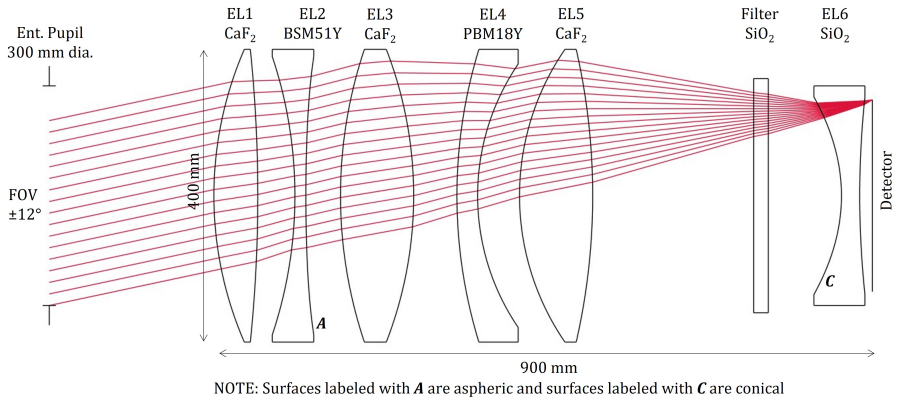

Figure 9: Optical layout of the WFOS red spectrograph camera prescription.

The red camera lens design (Fig. 9) is composed of two glass materials from the Ohara glass catalog: BSM51Y and PBM18Y, along with CaF_2 and SiO_2. The two Ohara glasses have been confirmed to be available in the

required blank sizes. The red camera prescription has a total of 6 lens elements with 1 aspheric surface located on lens element 2. The camera has an entrance aperture diameter of 400 mm and is ∼900 mm in length from the front surface vertex to the detector plane. The camera design delivers EE80 < 38 μm (0.″13) over an angular field of 24° for wavelengths ranging from 530 to 1050 nm. The maximum geometric vignetting is ∼ 11% at a field radius of 12° for a 300 mm circular pupil. The red camera has a passband-averaged transmission of ∼ 92% including bulk material absorption losses and Fresnel losses (assuming a 0.5% loss per surface).

3.4.3 Gratings

Table 1: WFOS Gratings and Spectral Resolving Power*

Channel	Grating	λ_p^a (Å)	$\Delta\lambda^b$ (Å)	$f_{\rm bw}^c$	$\langle R\rangle^d$ (w= 0.″75)	AOI^e (deg)	Active Area (mm×mm)
Blue	VPH1210	3930	3180	> 1.0	1500	15.9	310 × 320
Blue	VBG2500	4000	1580	0.63	3110	25-40	310 × 370
Blue	VBG3600	3700	830	0.33	5210	38-44	310 × 430
Blue	VBG2700	4400	1100	0.44	4750	36-42	310 × 430
Red	VPH680	7360	5680	> 1.0	1520	16.6	310 × 320
Red	VBG1400	7400	2450	0.53	3590	25-40	310 × 370
Red	VBG2052	6000	1440	0.31	5140	36-42	310 × 430
Red	VBG1520	7300	1940	0.42	4630	34-44	310 × 430

* The first-light WFOS grating complement will be optimized in the next development phase.
a) Wavelength of peak diffraction efficiency.
b) Wavelength coverage for spectra of length 240mm (see Figure 3.)
c) Fraction of the full channel bandwidth covered by a single grating setting.
d) Resolving power for entrance slit width w =0.″75; for other slit widths, multiply by 0.″75/w.
e) Angles of incidence over useful wavelength range.

The opto-mechanical layout of WFOS, with control over both grating tilt relative to the collimated beam axis (i.e. AOI at grating face) and the range of diffraction angles received by the cameras, allows for the use of any type of grating used in transmission. Although the grating suite to be delivered with the instrument for first light will be finalized in the next phase of development, we have produced an initial set of designs for both VPH and VBG gratings for each of 3 spectral resolution options in each channel. For the R∼1500 mode, which captures the full bandwidth of each wavelength channgel in a single exposure, we find that VPH gratings provide the best overall diffraction efficiency, even accounting for their sensitivity to changes in AOI for a wide-field imaging spectrograph (AOI ranges ±2.5° at the grating face). For moderate resolution modes where the ratio of the center wavelength to the groove spacing of the grating are near unity (λ_p/d∼1), the volume binary gratings provide higher diffraction efficiency (> 70%) over a much larger wavelength range and are far less AOI-dependent than an equivalent VPH grating; thus, we have adopted VBG designs as optimal for both the R∼3500 and R∼5000 spectral resolution modes. The initial set of gratings is summarized in Table 1, where the grating name indicates the technology (VPH or VBG) and the line density (mm^{-1}). The same gratings are used for the predictions of end-to-end instrumental throughput (§3.4.5 and Fig. 10.)

3.4.4 Detector Systems

As the f/2 spectrograph cameras on both the red and blue wavelength channels re-image the telescope focal surface with a final plate scale of 0.291 mm/″, the detector mosaics that capture the full field of view of WFOS must be at least 150 mm in the spatial (slit) direction, and 250 mm in the dispersion direction. Thus, assuming 15 μm pixels, the CCD mosaics must be at least 10k (spatial) by 17k (spectral) to capture the full camera field of view (Fig. 3). We have considered a number of mosaic configurations, accounting for the desire to use the same format on both wavelength channels so that gaps in the spatial (Y direction in Fig. 3) are aligned with one another, and to be able to optimize the CCD properties for blue or red sensitivity. The latter drives us toward thick ($\gtrsim$ 200 μm), fully depleted Si for the red channel, and thinned Si for the blue channel. Also taken

into account is the desire to minimize gap sizes between detectors in the spectral and spatial directions, and the ability to read out the full mosaic (binned 2×2) with read noise < 3 e$^-$ rms in <10 s.

3.4.5 Predicted Spectroscopic Throughput

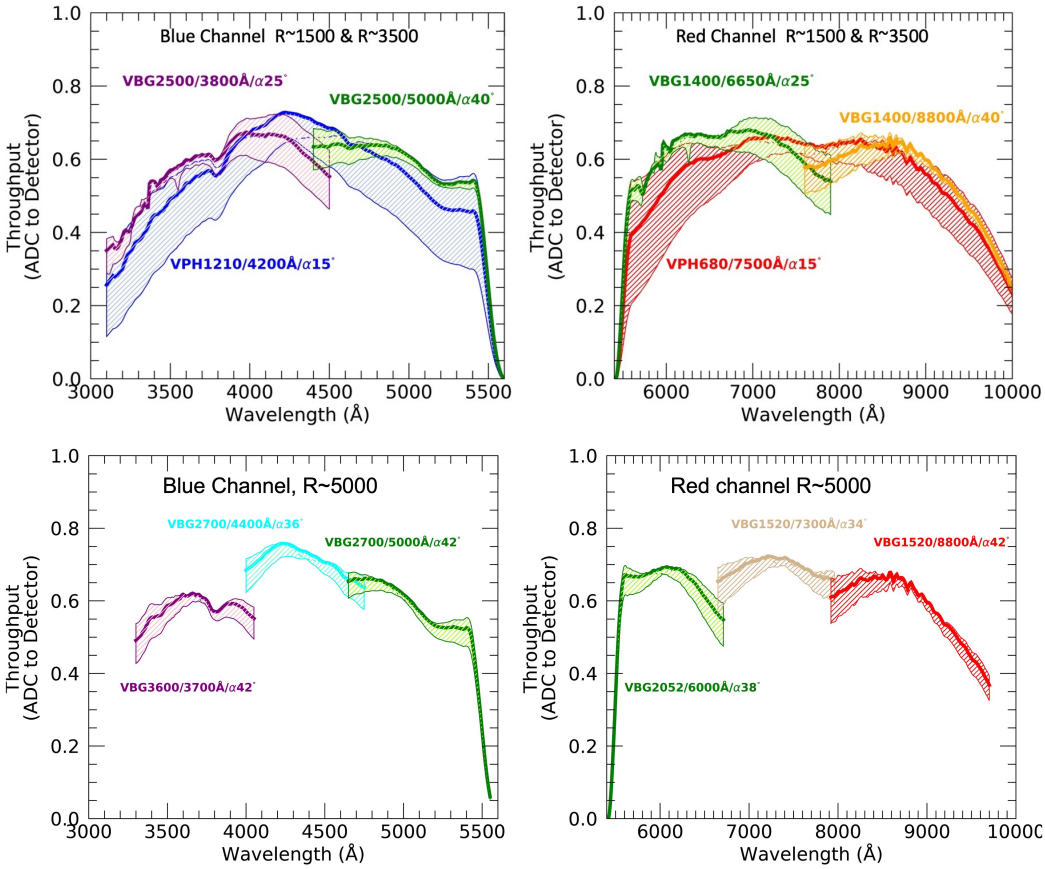

Figure 10: *Top:* Estimated throughput for WFOS blue and red wavelength channels, including the ADC to the detector, for the low-resolution ($R = 1500$) and medium-resolution ($R \sim 3500$) spectroscopic modes with gratings indicated (see Table 1.) The low-resolution curves assume a fixed AOI that centers the channel bandpass on the detector for a slit at the center of FoV. The throughput curves for the $R \sim 3500$ mode are shown for two different central AOI for the medium-resolution VBG gratings in Table 1, optimized for either the short wavelength or long wavelength half of the wavelength channel. The hatched regions in each panel show the range of efficiency curves that would apply to slits located at $X = \pm 1\farcm5$ from the field center, with the central AOI fixed. *Bottom:* Total throughput estimates assuming the 2 high- resolution ($R \sim 5000$) VBG gratings for each channel listed in Table 1. Each panel shows 3 different combinations of grating and central AOI, depending on wavelength. The dichroic split near 5600 Åis evident in each panel.

Fig. 10 shows the predicted instrument throughput for the gratings summarized in Table 1 at fixed central angles of incidence. These estimates include all transmission and reflection losses from the optical components, the grating efficiency modeled using Rigorous Coupled Wave Analysis (RCWA) numerical calculations, and the CCD quantum efficiency for currently-available detectors. The end-to-end efficiency of WFOS peaks near 70%, with passband-averaged values of $> 56\%$ for both blue and red wavelength channels.

4. SPECTROGRAPH BLUE AND RED CHANNEL ASSEMBLIES

Fig. 11 shows a CAD rendering of the optical bench that supports the blue channel spectrograph optics and mechanisms; the red channel optical bench, located below the blue channel on the rotating instrument structure, is identical except for the camera barrel and its support. The camera articulation stage, grating exchange

mechanism, and grating tilt mechanism are based on similar designs implemented for the KCWI instrument at the Keck Observatory 3, including the gravity-invariant layout.

The camera barrel, filter exchanger, detector cryostat, and LN_2 reservoir are mounted as a single assembly on the camera rotation stage, which is capable of rotating over an arc of $\sim 100°$ to accommodate the various observing modes (direct imaging, low, medium, and high resolution spectroscopy). The filter exchanger is integral to the camera system, providing a standard set of broadband filters for direct imaging and space for a small number of custom filters. Interference filters may also be placed at the pupil position in place of a diffraction grating by installing in a grating holder within the grating exchange system. The grating exchange system is designed to carry up to 10 gratings of active area size up to 310×430 mm^2, allowing for the addition of custom gratings in addition to those anticipated at first-light (Table 1.)

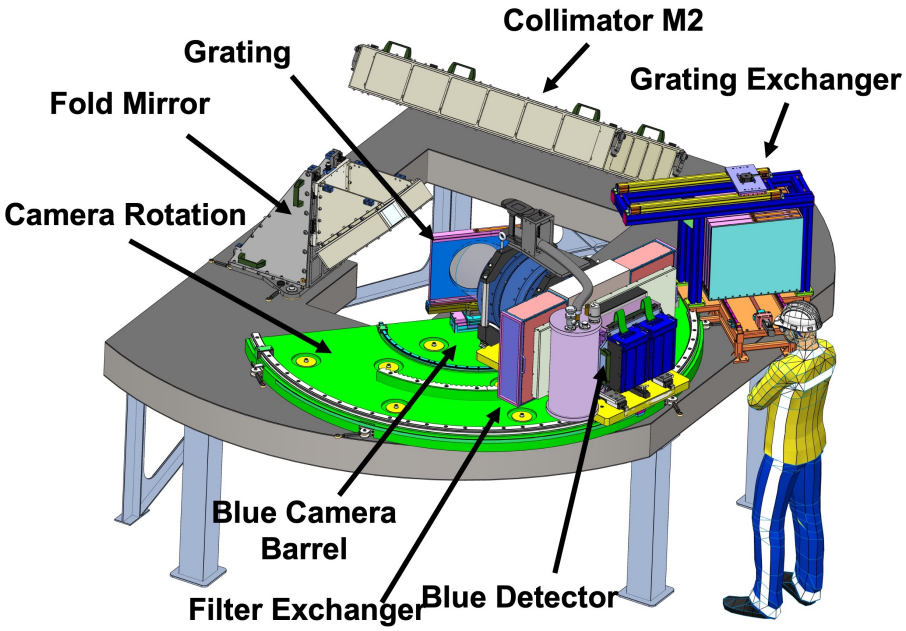

Figure 11: CAD rendering of the blue channel spectrograph assembly, including the camera rotation system, grating rotator, grating exchange system, and filter exchange system, along with the camera lens barrel and detector cryostat.

5. CALIBRATION SYSTEM

The large telescope aperture and compact dome of TMT makes it impractical to obtain daytime calibrations using illumination of a calibration screen inside the dome, imaged through the telescope optics. Instead, daytime calibrations, including both spectroscopic flat fields and comparison line lamps for wavelength calibration, are obtained using a separate calibration system. Light sources within a 1.5 m diameter integrating sphere pass through a simple optical system and then are reflected downward by M4 to illuminate the large WFOS focal plane (in physical units, $\sim 1.1\times0.4$ m^2) at f/15, thereby simulating sky illumination through the telescope optics.

6. UPGRADE PATHS

6.1 Slicer Integral Field Unit

The WFOS baseline design does not include an Integral Field Unit (IFU), but the instrument is designed with the explicit requirement to allow the future upgrade of the instrument with an IFU. To this end, the rotating structure includes an extra optical bench, just below the focal surface, to support a deployable image slicer system and its pupil relay optics (see second bench from top in Fig. 2). This upgrade will allow WFOS to obtain spectra of contiguous regions of the sky with an IFU that forms a virtual slit for each slice at the telescope focal surface.

The IFU concept is being developed by S. Ozaki and T. Tsuzuki (NAOJ). It is based on IFUs having 18 slices of length $20''$ each. With relay optics that provide a magnification of $1.1\times$, and with options for 4 different

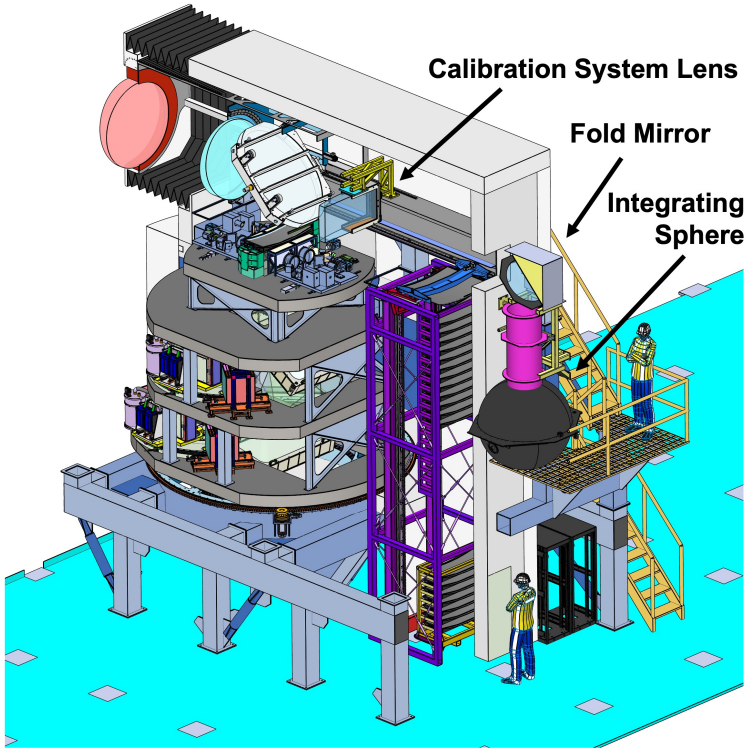

Figure 12: Schematic illustration of the WFOS calibration system, which is mounted to the non-rotating WFOS structure. Light is emitted from a 1.5m integrating sphere whose output is directed upward and then laterally toward M4, which rotates by 90 degrees with respect to its normal orientation receiving light from the ADC. A simple set of optics reimages the output of the integrating sphere to produce uniform illumination with an f/15 beam at the slitmask to simulate telescope illlumination. The illumination sources within the integrating sphere include continuum (LED) lamps for flat fields and line lamps for wavelength calibration.

slice widths (1.″5, 0.″75, 0.″5, or 0.″25), WFOS will record field sizes of 20″ × [27.″0, 13.″5, 9.″0, or 4.″5]. The finest slicer scale, in combination with the low-resolution (R∼1500) gratings discussed above, would provide complete wavelength coverage over the range 310 to 1050 nm with spectral resolving power R≃4000. If the R∼5000 grating is used, the resolving power can reach R≃14,000 in two simultaneous wavelength intervals (one blue, one red), each covering ∼30-40% of the full channel bandwidth.

6.2 Ground Layer Adaptive Optics

A requirement for WFOS is to ensure that the instrument is capable of being used in combination with ground-layer-adaptive optics-enhanced image quality delivered with a TMT facility GLAO system using an adaptive secondary mirror (ASM). Thus, the optics were specified for preserving the spectral resolution and image quality for entrance slits and point source PSFs down to angular sizes of 0.″25. In addition, the design of the WFOS AGWFS includes a preliminary design for laser guide star wavefront sensors assuming a LGS asterism consisting of 4 beacons in a rectangular configuration, 4.′6×5.′6, centered on the WFOS FoV (see Figs. 1 and 6.)

7. STATUS

The WFOS design described in this paper successfully passed its Conceptual Design Review in February 2022. The instrument is now in the Preliminary Design Phase. No major changes to the design described in this work are expected, with the possible exception of using a configurable slit unit in place of the slitmask exchange system that has been part of the design to date. A scientific and operational trade study for the focal plane mask architecture is ongoing at the time of writing. The WFOS schedule, including completion of the current Preliminary Design Phase, is on track for delivery to the TMT Observatory for first-light science.

ACKNOWLEDGMENTS

The TMT Project gratefully acknowledges the support of the TMT collaborating institutions. They are the California Institute of Technology, the University of California, the National Astronomical Observatory of Japan,

the National Astronomical Observatories of China and their consortium partners, the Department of Science and Technology of India and their supported institutes, and the National Research Council of Canada. This work was supported as well by the Gordon and Betty Moore Foundation, the Canada Foundation for Innovation, the Ontario Ministry of Research and Innovation, the Natural Sciences and Engineering Research Council of Canada, the British Columbia Knowledge Development Fund, the Association of Canadian Universities for Research in Astronomy (ACURA), the Association of Universities for Research in Astronomy (AURA), the U.S. National Science Foundation, the National Institutes of Natural Sciences of Japan, and the Department of Atomic Energy of India.

REFERENCES

[1] Phillips, A. C., Miller, J., Cowley, D., and Wallace, V., "The Keck-I Cassegrain ADC," in [*Ground-based and Airborne Instrumentation for Astronomy II*], McLean, I. S. and Casali, M. M., eds., *Society of Photo-Optical Instrumentation Engineers (SPIE) Conference Series* **7014**, 701453 (July 2008).

[2] Buchroeder, R. A., "Tilted-component telescopes. Part I: Theory.," *Applied Optics* **9**, 2169–2171 (Jan. 1970).

[3] Morrissey, P., Matuszewski, M., Martin, D. C., Neill, J. D., Epps, H., Fucik, J., Weber, B., Darvish, B., Adkins, S., Allen, S., Bartos, R., Belicki, J., Cabak, J., Callahan, S., Cowley, D., Crabill, M., Deich, W., Delecroix, A., Doppman, G., Hilyard, D., James, E., Kaye, S., Kokorowski, M., Kwok, S., Lanclos, K., Milner, S., Moore, A., O'Sullivan, D., Parihar, P., Park, S., Phillips, A., Rizzi, L., Rockosi, C., Rodriguez, H., Salaun, Y., Seaman, K., Sheikh, D., Weiss, J., and Zarzaca, R., "The Keck Cosmic Web Imager Integral Field Spectrograph," *Astrophysical Journal* **864**, 93 (Sept. 2018).